Solid-State Electronics Vol. 22, pp. 797–799

0038-1101/79/0901-0797/$02.00/0

SPATIAL RESOLUTION OF SEM-EBIC IMAGES

C. DONOLATO†
Max-Planck-Institut für Festkörperforschung, 7000 Stuttgart 80, Federal Republic of Germany

(*Received* 4 *August* 1978; *in revised form* 7 *March* 1979)

Abstract—Experiments indicate that the spatial resolution of SEM-EBIC images of semiconductor defects is not limited by the minority carrier diffusion length L. It is shown that this property can be explained by a three-dimensional analysis of the diffusion of beam generated minority carriers in a semiconductor having $L \to \infty$. For a small localized defect, the resolution is expected to be limited by the defect depth or the extension of the generation region, whichever is the greatest.

The electron beam induced conductivity (EBIC) mode of the scanning electron microscope (SEM) has been widely used for investigating the electrical activity of crystal defects in semiconductors, using a p–n junction[1, 2] or, more recently, a Schottky barrier[3, 4] to collect the beam generated carriers.

Relevant questions related to this method concern the dependence of the resolution of EBIC images on the shape of defects and their position relative to the surface, on the generation volume and possibly the minority carrier diffusion length in the bulk semiconductor. While the influence of the geometrical factors on the resolution seems to be well understood[3], there is still some difficulty in explaining the role played by the semiconductor diffusion length. In fact, it is generally assumed that carrier diffusion should cause an image broadening of the order of the diffusion length L; however, resolutions much better than L have been obtained experimentally[5, 7].

This note presents an argument to explain this contradiction, by taking into account the three-dimensional character of carrier diffusion. The derivation given below deals chiefly with small localized defects (i.e. defects that can be contained in a small sphere), but it will be shown that the argument also holds for extended defects like dislocations. The model applies to observations where a defect acts as a recombination site, thereby reducing the collected current; in some instances, however, as at high reverse bias of the collecting diode[8] or in bipolar transistors[9] enhancement of the EBIC signal at a defect is also possible.

The usual experimental arrangement for the Schottky barrier charge-collection to be discussed here is illustrated schematically in Fig. 1; similar considerations apply to a shallow p–n junction. The electron beam of the SEM is scanned over the surface of the diode and generates, through the thin metal electrode, electron-hole pairs in the semiconductor. The volume over which the generation is significant (the pear-like region about the beam axis in Fig. 1) has dimensions of the order of the range of incident electrons. In general, minority carriers will be generated both within the depletion layer of the diode at $0 < z < W$ and in the neutral region at $z > W$.

We suppose that a localized defect F is present in the neutral region, where minority carriers move only by diffusion; this location of the defect, therefore, should give the greatest diffusion broadening of the image. To prove that the resolution of the corresponding EBIC image is not limited by L, we shall consider the limiting case of $L \to \infty$ and show that, even with this extreme hypothesis, the resolution can be good. We shall do this by showing that the EBIC signal of the defect still decreases rapidly as the beam moves away from the defect. The problem of the charge collection at a defect when L is finite requires a more elaborate analysis and has been discussed elsewhere[10].

The defect is described as a region F where the lifetime of minority carriers (for instance holes in an n-type semiconductor) has a constant value τ_F. The assumption of $L \to \infty$ entails neglecting hole recombination in the bulk outside F and, therefore, also in the depletion layer. Let $g(\mathbf{r})$ be the electron-hole generation rate per unit volume due to the electron beam; the steady state continuity equation for the excess hole concentration $p(\mathbf{r})$ in the half-space $z \geq 0$ is then

$$(1/q)\,\mathrm{div}\,\mathbf{J}_p = g(\mathbf{r}) - (1/\tau_F)p(\mathbf{r})e(\mathbf{r}) \qquad (1)$$

where q is the magnitude of electronic charge, $\mathbf{J}_p$ is the hole current density and $e(\mathbf{r})$ is a function with value one inside F and zero outside. Integrating eqn (1) in the half-space $V(z \geq 0)$ and applying the divergence theorem we obtain

$$-\iint_{z=0} J_{pz}\,\mathrm{d}x\,\mathrm{d}y + \int_\Sigma \mathbf{J}_p \cdot \mathrm{d}\boldsymbol{\sigma} = q\int_V g(\mathbf{r})\,\mathrm{d}V - (q/\tau_F)\int_F p(\mathbf{r})\,\mathrm{d}V \qquad (2)$$

where Σ is the surface of the half-sphere at $r = \infty$. The first term on the left side of eqn (2) is the total collected current I; the integral over Σ vanishes, since J_p goes to zero at least as $1/r^3$ (this can be seen, for instance, by

†On leave from: C.N.R.-LAMEL, Via Castagnoli 1, 40126 Bologna, Italy.

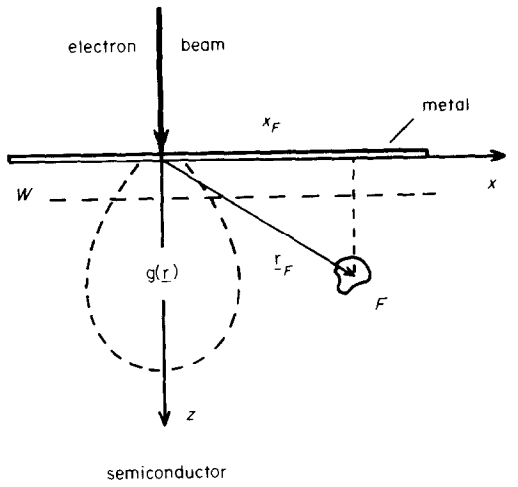

Fig. 1. Schematic illustration of the Schottky barrier EBIC imaging of a localized defect.

calculating $\mathbf{J}_p = -qD\nabla p$ with the aid of the dipole approximation for $p(\mathbf{r})$ as given in eqn (8)). We may then write

$$I = qG - q(V_F/\tau_F)\bar{p}_F = qG - I_F \tag{3}$$

where G is the total generation rate, V_F is the volume of the defect and $\bar{p}_F$ is the mean value of $p(\mathbf{r})$ inside F.

The term denoted by I_F in eqn (3) represents the decrease of the collected current brought about by the defect, i.e. the EBIC signal by which the defect is imaged. A first approximation for this term may be obtained by replacing, inside F, the unknown hole distribution $p(\mathbf{r})$ with $p^0(\mathbf{r})$, the distribution in absence of the defect. This approximation is expected to be adequate when I_F is small in comparison with the background current qG, that is for low-contrast defects, which is the most frequent practical case[4]. Moreover, if the defect dimension is much smaller than its depth, $p^0(\mathbf{r})$ will be approximately constant inside F, so that we have $\bar{p}_F \simeq \bar{p}_F{}^0 \simeq p^0(\mathbf{r}_F)$, $\mathbf{r}_F$ denoting the position of the defect. Equation (3) then gives

$$I_F \simeq q(V_F/\tau_F)p^0(\mathbf{r}_F). \tag{4}$$

To determine the hole distribution $p^0(\mathbf{r})$ in the bulk of the semiconductor ($z \geq W$) we have to solve a steady state diffusion equation, which can be written, in the limit $L \to \infty$, as

$$\nabla^2 p^0(\mathbf{r}) = -\frac{1}{D} g(\mathbf{r}) \tag{5}$$

where D is the hole diffusion coefficient. The boundary condition at the edge of the depletion layer is

$$p^0(\mathbf{r})|_{z=W} = 0. \tag{6}$$

Equation (5) is analogous to the Poisson's equation of electrostatics; with the boundary condition (6) it can be solved by the method of images[11], and the solution is

$$p^0(\mathbf{r}) = \frac{1}{4\pi D}\int_{z \geq W}\left(\frac{1}{|\mathbf{r}-\mathbf{r}'|} - \frac{1}{|\mathbf{r}-\mathbf{r}''|}\right) g(\mathbf{r}')\,\mathrm{d}V' \tag{7}$$

$\mathbf{r}''$ defining the image point of $\mathbf{r}'$ relative to the plane $z = W$. Since $g(\mathbf{r}')$ has cylindrical symmetry about the z axis, $p^0(\mathbf{r})$ will have the same symmetry, so that for a given defect depth $p^0(\mathbf{r})$ and hence I_F (eqn 4) will only be functions of the beam-defect horizontal distance x_F. The resolution of the image can be taken equal to the half-width w of the current profile $I_F(x_F)$, or equivalently of the hole distribution $p^0(x_F)$.

To show that a finite (and small) value of w is to be expected, we prove that $p^0(x_F)$ rapidly approaches zero as x_F increases. Since $g(\mathbf{r}')$ is essentially different from zero only inside a region with dimensions of the order of the primary electron range R_p, for $r \gg R_p$ we may apply to eqn (7) the well-known dipole approximation of electrostatics[11]; this yields $p^0(x_F) \sim 1/x_F{}^3$ for large x_F.

To give an estimate of the actual resolution when $L \to \infty$ and to point out which are the resolution limiting factors, we consider the case of a defect lying at a depth $a \gg W$, but still within the maximum range of primary electrons. This situation can be found in low resistivity semiconductors; for instance, in 1Ω cm p-type silicon W is about equal to 0.3 μm and a defect at a depth $a =$ 3 μm would be within the generation volume when $R_p >$ 3 μm, i.e. for electron beam energies $E > 20$ keV[3]. It is convenient to discuss separately the cases where R_p is small in comparison to a and where R_p is about equal or greater than a.

(a) $R_p \ll a$ but still $R_p > W$ in order to produce some contrast in the image. Since $a \gg R_p$, we have also $r_F \gg R_p$ for any x_F and the dipole approximation for eqn (7) holds; this yields

$$p^0(x_F) \propto a(a^2 + x_F^2)^{-3/2} \tag{8}$$

The half-width of this distribution is $w \simeq 1.5a$; for the above example this gives $w \simeq 4.5$ μm.

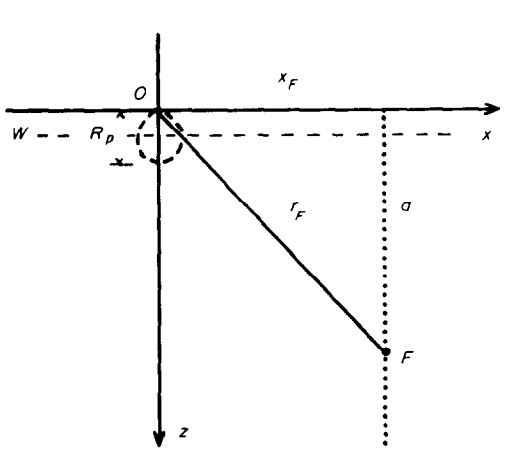

Fig. 2. Schematic diagram of the geometrical relations for the case of $R_p \ll a$. The same diagram is relevant for the imaging of dislocations.

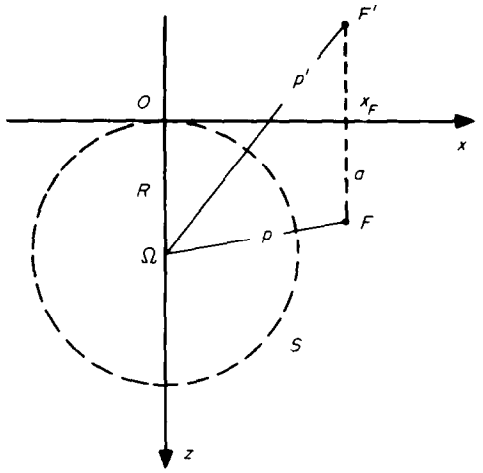

Fig. 3. Schematic diagram of the geometrical relations for the case of $R_p = 2R \geq a$.

(b) $R_p \geq a$. To estimate the resolution in this case, we suppose, as is frequently done[5, 12], that $g(\mathbf{r}')$ is constant inside a sphere S of radius $R = R_p/2$ tangent to the surface and equal to zero outside. Being $a \gg W$ we have now $R_p \gg W$ and the generation sphere S can be considered to lie entirely in the neutral region. Thus the integral in eqn (7) reduces to well-known integrals of electrostatics, whose evaluation yields

$$p^0(x_F) \simeq (G/4\pi D) \cdot \begin{cases} (1/\rho) - (1/\rho') & \text{if } \rho \geq R \\ (1/2R)[3 - (\rho/R)^2] - (1/\rho') & \text{if } \rho \leq R \end{cases} \quad (9)$$

where ρ and ρ' are the distances of F and its image F' to the centre Ω of S, respectively (Fig. 3). By expressing ρ and ρ' through R, a and x_F, an explicit form for $p^0(x_F)$ can be obtained. A numerical evaluation of the half-width of this distribution shows that $w \simeq 2R = R_p$ when $R_p \geq a$.

Thus, according to the present model, the resolution limiting factors in the EBIC imaging of small localized defects are the defect depth or the extension of the generation region, whichever is the greatest. For the previous example of a defect at a depth $a = 3\,\mu$m this means that for $E > 20$ keV a resolution approximately equal to the corresponding range should be obtained; decreasing the beam energy well under 20 keV should not improve any further the resolution, which should remain about equal to 4.5 μm.

The main argument about resolution can be easily extended to the case of a dislocation, by representing this defect as a continuous distribution of point-like defects on a line. We consider here the simplest case of a straight semi-infinite dislocation perpendicular to the surface, which is represented as a dotted line through F in Fig. 2. For $x_F \gg R_p$ the dipole approximation holds for any a and relation (8) can be applied to the single points of the dislocation. Apart from constant factors, the EBIC signal of a dislocation $I_D(x_F)$ for large x_F is then found by integrating eqn (8) with respect to a from zero to infinity; the integration is immediate and gives $I_D(x_F) \sim 1/x_F$. This result indicates that the EBIC signal due to a dislocation is still going to zero as $x_F \to \infty$, although not so strongly as in the case of a localized defect. Thus good resolution is also to be expected in the EBIC images of dislocations in a semiconductor with $L \to \infty$; further properties of dislocation images are considered in Ref.[13].

The present discussion has been concerned with the EBIC imaging mode of defects, but it is thought that the main conclusions about resolution apply to the CL (cathodoluminescence) imaging mode as well. In fact, in both modes a defect is imaged because it enhances locally the recombination (the non-radiative recombination, in the case of CL) of beam generated carriers. Since the recombination rate at a defect is proportional to the excess minority carrier density at that point, both the EBIC and the CL signals decrease with the beam-defect distance as the minority carrier concentration does. The three-dimensional character of carrier diffusion is therefore equally relevant for the two methods and consequently similar resolution properties of EBIC and CL images are expected.

Acknowledgements—The author wishes to thank Prof. H. J. Queisser for his advice and encouragement; he is also grateful to the Max-Planck-Gesellschaft for the award of a research fellowship.

REFERENCES

1. K. V. Ravi, C. J. Varker and C. E. Volk, *J. Electrochem. Soc.* **120**, 533 (1973).
2. D. B. Holt and R. Ogden, *Solid-St. Electron.* **19**, 37 (1976).
3. H. J. Leamy, L. C. Kimerling and S. D. Ferris, *Scanning Electron Microscopy*, 1976, Chicago, p. 529. IIT Research Institute (1976).
4. R. B. Marcus, M. Robinson, T. T. Sheng, S. E. Haszko, S. P. Murarka and L. E. Katz, *J. Electrochem. Soc.* **124**, 425 (1977).
5. S. M. Davidson, *J. Microsc.* **110**, 177 (1977).
6. D. B. Darby and G. R. Booker, *J. Mater. Sci.* **12**, 1827 (1977).
7. D. E. Ioannou and S. M. Davidson, *Phys. Stat. Sol.* (*a*) **48**, K1 (1978).
8. A. J. Gonzales, *Scanning Electron Microscopy*, 1974, Chicago, p. 942. IIT Research Institute (1974).
9. P. Ashburn and C. J. Bull, *Solid-St. Electron.* **22**, 105 (1979).
10. C. Donolato, *Optik* **52**, 19 (1978).
11. See e.g.: W. K. H. Panofsky and M. Phillips, *Classical Electricity and Magnetism*. Addison-Wesley, Reading, Mass. (1962).
12. F. Berz and H. K. Kuiken, *Solid-St. Electron.* **19**, 437 (1976).
13. C. Donolato, *Appl. Phys. Lett.* **34**, 80 (1979).